Food Hydrocolloids 71 (2017) 35–46

Contents lists available at ScienceDirect

Food Hydrocolloids

journal homepage: www.elsevier.com/locate/foodhyd

Polysaccharide blended whey protein isolate-(WPI) hydrogels: A physicochemical and controlled release study

Baris Ozel [a, b], Sevil Cikrikci [b], Ozlem Aydin [a], Mecit Halil Oztop [b, *]

[a] Food Engineering Department, Ahi Evran University, Kirsehir, Turkey
[b] Food Engineering Department, Middle East Technical University, Ankara, Turkey

ARTICLE INFO

Article history:
Received 28 December 2016
Received in revised form
13 April 2017
Accepted 21 April 2017
Available online 28 April 2017

Keywords:
Hydrogel
Swelling
Release
IR-microwave
NMR
SEM

ABSTRACT

Design and characterization of composite whey protein isolate (WPI) hydrogels are gaining interest due to their utilization as controlled delivery matrices for bioactive agents. In this study, black carrot extract (BC) loaded composite WPI hydrogels, containing xanthan (XN), pectin (PC) and gum tragacanth (GT) were prepared by conventional water bath (CV) and infrared (IR) assisted microwave heating (MW). Release and swelling experiments were conducted at pH 7.0 phosphate buffer solution for 24 h. Highest swelling ratio (SR) was observed at CV XN hydrogels and only XN hydrogels showed a distinct increase in SR (17.85%) with respect to WPI hydrogels containing no additional polymer (10.55%) ($p < 0.05$). CV WPI hydrogels having no added polysaccharide showed the highest release percent (77.81%). CV PC, XN and GT hydrogels with release ratios of 37.15%, 32.79% and 29.39%, respectively, were capable of retarding release with respect to sole WPI hydrogels ($p < 0.05$). MW increased the release rates of all polymer added hydrogels. Nuclear Magnetic Resonance (NMR) relaxometry was used to understand the polymer-water interactions in the samples. Therefore, transverse relaxation times (T_2) and self-diffusion coefficients (SDC) of each hydrogel were measured. Increasing T_2 and SDC values of CV XN samples were associated with better gel characteristics. Scanning electron microscope (SEM) images revealed the microstructural differences between the heating and polymer types. Mathematical modelling of release behaviors of hydrogels was also conducted to estimate diffusion coefficients. Moreover, this study introduces the effects of MW-IR heating on the physiochemical and controlled release behavior of WPI-GT composite hydrogels for the first time.

1. Introduction

Hydrogels are three-dimensional networks of natural or synthetic polymers with the ability of absorbing large amounts of water by either physical or chemical crosslinking (Argin, Kofinas, & Lo, 2014; Kim, Flamme, & Peppas, 2002). They get great attention in encapsulated delivery systems, for delivery of therapeutic drugs and bioactive components to the site of interest leading great applications in biotechnology, medicine and food technology (Belscak-Cvitanovic et al., 2015). In recent years, various hydrogels, particularly from proteins (Betz & Kulozik, 2011b) and polysaccharides like rice starch (Mun, Kim, & McClements, 2015), alginate (Wichchukit, Oztop, McCarthy, & McCarthy, 2013), chitosan (Lu et al., 2015) and pectin (Luqin et al., 2009) as food grade polymers have been used as delivery matrices for active agents owing to their biodegradability, biocompatibility and nontoxicity features. Moreover, the combined use of protein and polysaccharides is of high interest for development of novel gel systems since different polysaccharides interact variously with the protein network, giving control over manipulating release rates of such gels.

One of the most common food proteins for gel formulation is whey protein (WP) (Betz & Kulozik, 2011b). Several studies have been conducted about WP hydrogels due to their potential for controlled release applications (Betz & Kulozik, 2011a; Betz et al., 2012; Gunasekaran, Ko, & Xiao, 2007). WP is capable of forming heat-set gel matrixes, having the ability to absorb large amounts of water and entrap active agents for delivery (Oztop, McCarthy, McCarthy, & Rosenberg, 2012). WP mainly consists of globular proteins β-lactoglobulin (β-Lg, ~65% w/w) and α-lactalbumin (α-La,

* Corresponding author. Middle East Technical University (METU), Universiteler Mah., Dumlupinar Bulvari, No: 1 Cankaya, 06800, Ankara, Turkey.
E-mail addresses: bozel@metu.edu.tr (B. Ozel), cikrikci@metu.edu.tr (S. Cikrikci), ozlem.aydin@ahievran.edu.tr (O. Aydin), mecit@metu.edu.tr (M.H. Oztop).

http://dx.doi.org/10.1016/j.foodhyd.2017.04.031
0268-005X/

~25% w/w), which are responsible for gelling, emulsifying, foaming properties and hydration capacity of WP (Shiroodi, Rasco, & Lo, 2015). WP gelling is obtained by an aggregation process induced by changing conditions usually by increase in temperature. Heat-induced gel is formed by thermal (partial) unfolding of native proteins which leads to exposure of non-polar residues, and this causes clustering of aggregates for a spatial gel network formation (Munialo et al., 2016).

WP gelling is mainly achieved by conventional heating above its thermal denaturation temperature (McClements, 2017). Microwave heating (MW) might be considered as an alternative method for conventional heating (CV) gelation process. Microwaves are oscillating electromagnetic waves in the frequency range of 300 MHz and 300 GHz on the material, causing an instantaneous heat generation due to the polarization of the chemical constituents in the material (Liu & Kuo, 2011). It reveals distinct advantages and is widely accepted by food industry. MW offers faster heating time, energy efficiency, precise process control and selective heating (Aydogdu, Sumnu, & Sahin, 2015; Turabi, Sumnu, & Sahin, 2010). There exists less time for formation of three dimensional gel matrix and it affects gel properties. It could lead weaker and coagulate-like structures in gels (Gustaw & Mleko, 2007). Combining MWs with other modes of heating such as near infrared heating (IR) could also provide more control on moisture transport by increasing heating rate (Turabi et al., 2010). There are some studies conducted to see the effect of microwave heating on protein gelation. They reveal that heating process is among the factors influencing gel matrix. Gustaw and Mleko (2007) compared both conventional and microwave heating on whey protein gelation at different pH values. Similarly, Liu and Kuo (2011) analyzed microstructure and rheological properties of soy protein isolate gel produced by microwave heating formation. However, applying IR-assisted MW on WP based gel processing was aimed in this research to investigate the performance of different heating types on gelation process.

In recent years, the interest to study the behavior of synergistic interaction of proteins with various polysaccharides has increased to diversify functional properties of gels (Betz & Kulozik, 2011a; Betz et al., 2012; Mun et al., 2015; Petzold et al., 2014; Wichchukit et al., 2013; Zhang, Andrew, & McClements, 2014). Gum types could modulate functional and microstructural properties of WP gels through duplex formation creating features of interest for novel applications (Zand-Rajabi & Madadlou, 2016). The nature of interactions (attractive or repulsive) between two polymers causes different behaviors like associative phase separation or co-solubility forming soluble/insoluble complexes and consequently complex formation gives different functional properties than polysaccharides and proteins alone (Shiroodi, Mohammadifar, Gorji, Ezzatpanah, & Zohouri, 2012). Mixed gels reveal opportunity to enhance structural characteristics of gel systems or to offer novel functions as carrier system for several active agents. Biopolymer nature, protein to polysaccharide ratio, biopolymer concentration and ionic strength are among the factors affecting gel properties (Le, Rioux, & Turgeon, 2016).

Pectin (PC) is a negatively charged, nontoxic, biodegradable biopolymer which is comprised of galacturonic acid and partially methoxylated carboxyl groups (Tsai et al., 2014). Wide amount of hydroxyl and carboxylate groups in PC leads to high hydrophilicity which results in polymer chain extension by charge repulsion and a high water absorption (Guo & Kaletunc, 2016). Xanthan (XN) is another widely used anionic heteropolysaccharide adopting a double-strand helix conformation in its native state and including a cellulose backbone and trisaccharide side chains containing glucuronic acids and a pyruvate group. XN, widely used in food products as a thickener or stabilizer, has a rigid and rod-like structure and its high molecular weight up to 6 MDa creates a high viscosity solution even at very low concentrations. It could give response to external stimuli by exchanging intra- and intermolecular interactions inducing a variety of conformations. The rigid helix–coil structure transforms into flexible coils in solution in which pH and ionic environment influence physical properties and stability of XN (Mikac, Sepe, Kristl, & Baumgartner, 2010). Another polysaccharide, gum tragacanth (GT), also known as katira, is a branched, heterogeneous, and anionic carbohydrate polymer consisting of D-galactose, D-galacturonic acid, D-xylose, L-fucose, and L-arabinose units giving special functionalities (Shiroodi et al., 2012). It includes two major fractions as tragacanthin (water soluble) and bassorin (water swellable). Bassorin composes 60–70% of the total gum and has the abilities of swelling and gel forming (Mostafavi, Kadkhodaee, Emadzadeh, & Koocheki, 2016).

Rheological and release properties of WP mixtures with several polysaccharides such as gellan (Zand-Rajabi & Madadlou, 2016), XN-curdlan (Shiroodi et al., 2015), wheat starch (Yang, Luan, Ashton, Gorczyca, & Kasapis, 2014) and alginate (Déat-lainé et al., 2013; Leon, Medina, Park, & Aguilera, 2016) had been studied in literature before for various active agents.

Anthocyanins as bioactive plant phenolics are attractive functional food additives having beneficial health effects (Betz & Kulozik, 2011b; Betz et al., 2012). Black carrot (BC) is among the sources due to its high anthocyanin content (1.75 kg/kg) and extraordinary quality parameters (Khandare, Walia, Singh, & Kaur, 2011; Kirca, Ozkan, & Cemeroglu, 2006). Thus, the use of BC concentrate for release behavior contributes to attractiveness of this concept. Moreover, a study to see the influence of addition of PC, XN or GT to WP based hydrogels for entrapment of anthocyanin rich BC concentrate has not been encountered.

When hydrogels are placed in water, they usually swell owing to penetration of hydrophilic solvent resulting from polymer chain relaxation (Ozel, Uguz, Kilercioglu, Grunin, & Oztop, 2016). However, degree of protein-protein, protein-water or protein-ion interaction become important for the swelling response of each gel formulation (Oztop, McCarthy, McCarthy, & Rosenberg, 2014; Siepmann & Peppas, 2001). As well as swelling behavior, gel formulation and surrounding aqueous medium in which release occurs influence the release ability of hydrogels (Ozel et al., 2016; Siepmann & Peppas, 2001). Release of active agents from a gel could be explained by diffusion, swelling or chemical mechanisms (Lee & Rosenberg, 2000). When swelling has no effect on diffusion, diffusion controlled release could be expressed by Fick's law of diffusion. Swelling controlled release occurs on the condition that mass transfer of active compound is faster than swelling of gel (Oztop et al., 2014). Both diffusion and swelling related mechanisms may affect the release behavior in WP gels. There are also alternative models taking into account both diffusion by Brownian motion and polymer relaxation for prediction of molecule release; they may require several modelling iterations as a more rigorous method (Lin & Metters, 2006). Diffusion coefficient could be examined in terms of molecular motions; such kind of Brownian motion could arise from random motion of particles. This random motion then is connected to diffusion (Cussler, 2009). In another mechanism, chemically controlled release systems, reactions occur within delivery matrix such as cleavage of polymer chains via enzymatic or hydrolytic degradation, during the release of the encapsulated substance (Lin & Metters, 2006). In this study, a mathematical model for release behavior of hydrogels was also developed using Fick's law of diffusion to estimate diffusion coefficients of hydrogels formulated with different polymers.

Nuclear Magnetic Resonance (NMR) relaxometry is an alternative tool to comprehend swelling and release behaviors of polymer matrices. It allows identification of water distribution and molecular interactions of gums (such as polymer- polymer and polymer-

water interactions) without giving any damage to the sample (Williams, Oztop, McCarthy, McCarthy, & Lo, 2011). NMR enables the characterization of changes in conformation of biopolymer chains and mobility of protons through the transverse component of magnetization timse constant which is T_2 (Oztop et al., 2014). T_2 values of each gel system could give information about the solvent uptake characteristics of each gel. In addition to T_2 values, self-diffusion coefficient (SDC) of water in hydrogels can also be determined by NMR relaxometry since NMR is an effective tool to detect molecular mobility and can yield SDC from a macroscopic scale (Sun et al., 2016).

The main aim of the current study was to investigate solvent uptake and release behaviors of heat-set composite WP gels produced by different heating methods. WP hydrogels, as carrier systems, were combined with PC, XN or GT and a bioactive compound, BC concentrate, as a source of model bioactive agent. The influence of incorporating BC concentrate into WP based hydrogels mixed with different polysaccharides was examined with the help of both gravimetric and NMR methods. Moreover, the effects of gelation process induced by CV or IR assisted MW on release behaviors were evaluated for all formulations. The release and swelling results of hydrogels were also explained by the microstructural differences of hydrogels obtained by scanning electron microscope (SEM) images. The information obtained in this study could be useful for improvement of hydrogel formulations as delivery matrices for BC concentrate.

2. Materials and methods

The polysaccharides PC (FMC, Italy S.R.L.) and GT (C.E. Roeper GmbH, Hamburg, Germany) were kindly provided by FMC group (FMC BioPolymer, Philadelphia, USA). XN (Smart Chemistry and Dan. Ltd. Co, Izmir, Turkey) was purchased as the final polysaccharide to be used in the experiments. Whey protein isolate (WPI) with protein content of 88.5% determined by Kjeldahl method was used as the main gelling ingredient (Hardline Nutrition, Kavi Food Ltd. Co., Istanbul, Turkey). BC concentrate having a total phenolic content and antioxidant activity of 20.588 mg Gallic Acid Equivalent (GAE)/g sample and 1.926 mg 2,2-diphenyl-1-picrylhydrazyl (DPPH)/g sample, respectively, was provided from Targid A.S. (Targid Agriculture Co. Inc., Icel, Turkey).

2.1. Gel preparation

The preparation of hydrogels was carried out by heat gelation. They were formulated with three different gums; PC, XN, GT, and a control sample without gum (C) was also prepared. The solution consisted of 15% (w/w) WPI, 0.5% (w/w) gum, 4% (w/w) BC concentrate as the target active agent, 0.02% (w/w) sodium azide (Merck KgaA, Darmstadt, Germany) as the antimicrobial agent and 80.48% (w/w) distilled water. The amounts of WPI, gum and BC concentrate were determined by preliminary experiments and optimized for the study. Firstly, WP solutions without BC and gum solutions containing BC were stirred at 15,000 rpm for 2 min using Ultra Turrax T-18 (IKA Corp., Staufen, Germany) separately and then combined in a beaker at the magnetic stirrer. Polymer solutions were left on the magnetic stirrer overnight at room temperature. Only XN solutions were centrifuged at 715.52 *g* for 2 min (Hanil Science Industrial Co., Ltd., Incheon, Korea) after overnight stirring to remove excess air bubbles present in XN solutions. The pH of resulting solutions of PC, XN, GT and C were in the range between 5.66 and 5.89. Gelation was conducted by two different ways; in water bath (Wisd, Wertheim, Germany) at 90 °C for 30 min as CV or in IR-assisted MW oven consisting of two upper and one lower halogen lamp, a turntable and a microwave source (General Electric Company, Louisville, KY, USA). Microwave oven had the cavity size of 21 cm height, 48 cm length and 33 cm height. The oven had a microwave power of 706 W which was determined by using IMPI 2-l test (Buffler, 1993). For IR-MW combination, the power levels of the upper and the lower halogen lamps (1500 W, each) as IR source were adjusted to 40% and the microwave power of 50% were used with approximately 2.5 min of heating time which was the minimum sufficient time for gelation of samples in MW oven. The minimum sufficient time for MW gelation was determined by preliminary experiments and heating over 2.5 min caused gels to burst and lose their gel structure due to excess internal water vaporization within the samples. Gel solutions which would be used for water bath process were poured into cylindrical glass tubes (5 cm long, 1.5 cm outer diameter). Other solutions that would be gelled in the microwave oven were poured into beakers having large cross sectional area (9.5 cm diameter) rather than glass tubes to prevent overflowing. Following gelation, gels in tubes/beakers were immediately cooled in ice water for 15 min. Finally, they were cut into 1.3 cm diameter cylindrical shapes having lengths of 2 cm.

2.2. Swelling study

Since samples gelled in microwave oven could not maintain their shape in swelling medium for 24 h, only samples gelled in water bath were analyzed for swelling study. The swelling behavior of gel samples was performed in phosphate buffer solution at pH 7.0. The reason for using neutral pH phosphate buffer solution was to mainly focus on the effect of temperature and heating type on the formation of biopolymer complexes rather than pH alteration effect. Biopolymer complexes are also formed at neutral pH and the ionic nature of phosphate buffer provides information about the behavior of biopolymers under such conditions. Cylindrical gels were placed in plastic mesh baskets and immersed into 150 ml buffer solution. They were allowed to swell at room temperature up to 24 h. The swollen gels were periodically (0.5, 1, 2, 3, 4, 5, 6 and 24 h) removed, blotted with filter paper to remove excess water and weighed immediately. Then, swelling ratio was calculated as:

$$\text{Swelling ratio } (\%) = ((Wt - Wo)/Wo) \times 100 \quad (1)$$

where Wt is the weight of gel at the defined time, Wo is the initial gel weight. All experiments were conducted in triplicate.

2.3. Release of black carrot concentrate from hydrogels

Release of BC concentrate through hydrogels was monitored by a UV–visible spectrophotometer (Mecasys Co. LTD, Korea) at determined time intervals (0.5, 1, 2, 3, 4, 5, 6, and 24 h). Gels (with 1.3 cm diameter, 2 cm length) were immersed into 40 ml phosphate buffer (at pH 7.0) stirring at 80 rpm. At specified times, 4 ml of buffer solution was withdrawn from the medium and absorbance was measured at 530 nm. Buffer solution was put back into the medium to keep medium volume constant. Calibration curve was made using known amounts of BC concentrate with respect to absorbance ($y = 7.5704x$-4E-05 where y and x represented absorbance and g BC/40 g buffer, respectively). To assess the stability of BC with respect to temperature, BC concentrate was exposed to heating conditions used in this study in preliminary experiments. The color of the concentrate was found to be stable within the time and temperature intervals of heating processes. The tests were conducted on three independent replicates.

2.4. NMR relaxometry measurements

NMR experiments were performed on a 0.32 T NMR system (Spin Track SB4, Mary El, Russia). For T_2 measurements each hydrogel was placed in the NMR instrument and Carr-Purcell-Meiboom-Gill (CPMG) sequence was used with 1 ms echo time, 400 echoes, 300 ms period with scan amount of 64. T_2 measurements of hydrogels were performed at determined time intervals (0, 2, 4, 6 and 24 h) of solvent uptake. SDCs of hydrogels were also measured by NMR for 0 and 6 h of the experiment. For self-diffusion experiments stimulated spin echo pulse sequence was used. Spin echo pulse sequence contained three 22 us, 90° pulses. The time intervals between the first and the second pulses and between the second and the third pulses were 2 ms and 60 ms, respectively, with an acquisition time of 500 us. The duration of the pulsed gradient field was 1 ms and the gradient strength was 1.66e-2 T/m.

2.5. Dielectric measurements

Dielectric properties (dielectric constant and dielectric loss factor) of solutions from which hydrogels would be obtained were determined by Agilent 85070E open-ended coaxial probe system connected to an Agilent E8362B Vector Network Analyzer (Agilent Technologies ES061B ENA Series Network Analyzer, USA).

2.6. Viscosity measurements

After the solutions are prepared through overnight stirring to let the full hydration of the polymers, viscosities of all gel solutions were measured. Viscosities of all gel solutions were measured with Sinewave Vibro Viscometer SV-10/SV-100 (A&D Company Limited, Japan) having two viscosity detecting gold covered sensor plates oscillating in opposite directions. Sensor plates have a low frequency of 30 Hz and an amplitude of less than 1 mm. Before measurements, samples were stabilized at 20 °C. Measurements were conducted in triplicate.

2.7. Scanning electron microscope

Samples undergoing SEM were first freeze dried (Christ, Alpha 2–4 LD plus, Germany) at 48 h after refrigeration period. Freeze dried gels were gold sputtered and then analyzed with a SEM (FEI Nova NanoSEM 430, Oregon, USA) at an accelerating voltage of 20 kV. Images were observed at magnification levels of 80×, 300×, and 10000×. Analyses were conducted at Metallurgical and Materials Engineering Laboratory of METU (Ankara, Turkey).

2.8. Modelling release behavior of gel samples

To calculate effective diffusion coefficient for release of BC concentrate from each gel sample with the shape of cylinder, mass transport equation for diffusion in infinite plane and infinite cylinder in a stirred solution of limited volume were combined with product rule. Thus, the solution for finite cylinder geometry satisfied the conditions of "product type solution" as given in the study of (Crank, 1975);

$$\frac{M_t}{M_{inf}} = 1 - \left(\sum_{m=1}^{\infty} \frac{4\gamma(1+\gamma)}{4+4\gamma+\gamma^2 q_m^2} exp\left(-\frac{Dq_m^2}{R^2}t\right)\right) \cdot \left(\sum_{m=1}^{\infty} \frac{2\gamma(1+\gamma)}{1+\gamma+\gamma^2 p_n^2} exp\left(-\frac{4Dp_n^2}{h^2}t\right)\right) \quad (2)$$

where M_t/M_∞ is the ratio of the diffusing agent at time t as fraction of the instantaneous uptake (Mt) to the uptake at long times (M_∞). R and h are the radius and height of the sample respectively. γ represents ratio of the volume of the solution to the volume of sample. *D* is the effective diffusion coefficient. The qm's are the nonzero positive roots of

$$\gamma q_m J_0(q_m) + 2J_1(q_m) = 0$$

and p_n's are the nonzero positive roots of

$$\tan(p_n) = -\gamma p_n$$

Experimental results were fitted to Eqn. (2) and diffusion coefficients were found by using MATLAB function "lsqnonlin".

2.9. Statistical analysis

Analysis of variance (ANOVA) was performed to determine whether there was a significant difference on measurements between hydrogel formulations and heating types. If significant difference was detected, means were compared by the Tukey test ($p < 0.05$) using MINITAB (Version 16) software.

3. Results and discussion

3.1. Swelling ratios

All hydrogels prepared by CV showed an increase in swelling ratio (SR) from the first 30 min to 24 h of the swelling experiment indicating that all samples absorbed and retained some amount of solvent within their gel structure. MW hydrogels could not maintain their structures in pH 7.0 phosphate buffer and degraded during 24 h swelling experiments. Clearly, MW hydrogels had weaker gel structures than CV heated ones. Thus, only the SR of CV samples were recorded. As shown in Fig. 1, XN hydrogels had the highest SR 17.85% at the end of 24 h and only XN samples differed from C samples which had the lowest SR 10.55%. The SR of PC and GT samples were somewhere between those two SR, 13.87% and 10.88%, respectively, so their SR did not show a significant increase compared to C sample ($p < 0.05$). These results suggest that addition of XN into the WPI hydrogel increased the swelling ability of that hydrogel. XN, having a high molecular weight of 2000 kDa, was known for its high water holding capacity and viscosity increasing properties (Garcia-Ochoa, Santos, Casas, & Gomez, 2000). Viscosity measurements of hydrogel solutions also proved that XN increased the solution viscosity substantially as shown in Table 1. XN was also

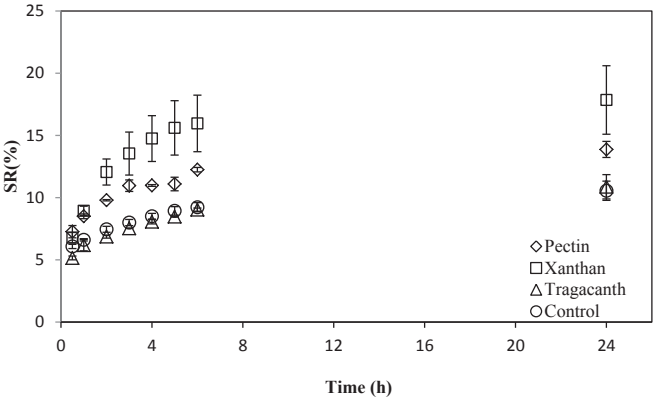

Fig. 1. Swelling ratio profile of conventionally heated hydrogels (0–24 h).

Table 1
Viscosity values of hydrogel solutions containing black carrot extract (mPa.s) at 20 °C. Errors are reported as the standard deviation between replicates. Different letters means viscosity values of samples differed significantly ($p < 0.05$). (Note: viscosity of distilled water at 20 °C is 1000 mPa s).

Hydrogel Solutions	Viscosity (mPa s)
Xanthan	122.000± 1.732[a]
Tragacanth	25.267± 0.152[b]
Pectin	14.000± 0.264[c]
Control	3.587± 0.025[d]

reported to reduce the syneresis in curdlan-WPI solution over freeze thaw cycles (Shiroodi, Rasco and Lo., 2015). The SR results of XN added hydrogels were in agreement with these studies. At pH 7.0, XN having β-D-glucose unit as a linear backbone, is negatively charged due to its trisaccharide side chain containing an acetylated mannose, glucuronic acid residue and a pyruvic acid residue or a mannose residue, alternatively (Zasypkin, Dumay, & Cheftel, 1996). WPI having a pI around 5.2 is also negatively charged at pH 7.0 and high electrostatic repulsion is expected in WPI-XN complexes (Hatami, Nejatian, Mohammadifar, & Pourmand, 2014). However, proteins have positively charged internal patches even at pH's higher than their pI and this makes possible for polysaccharide molecules to interact with WPI molecules in terms of electrostatic attractions. The large size and compact structure as well as the charge repulsion in the side chains of XN, induced solutions with high viscosity and resulting gels were also capable of retaining larger amounts of solvent with respect to C samples. This was expected because electrostatic repulsion of side chains contributes to solvent uptake characteristics (Hatami et al., 2014). PC is also a branched, heterogeneous, anionic and structurally complex polysaccharide as XN (Mohnen, 2008). The galacturonic acid backbone of PC has side chains called rhamnose rich regions carrying natural sugars such as galactose, arabinose and xylose (Ventura & Bianco-Peled, 2015). The main reason for the difference in SR of PC and XN hydrogels originates from the different kind of residues located in the side chains. Each residue has distinct charge, bond forming and electrostatic interaction capacities with the environment. It is hypothesized that charge repulsion between PC residues is lower than the charge repulsion between XN residues at pH 7.0 thus PC resulted in a lower SR. PC solution viscosity was also lower than XN solutions proving viscosity effect on SR (Table 1). GT which is a highly acid resistant and heat stable hydrocolloid, due to its easy separation procedures, is a physical mixture of tragacanthin (water-soluble) and bassorin (water-swellable) parts (Balaghi, Mohammadifar, Zargaraan, Gavlighi, & Mohammadi, 2010). Balaghi, Mohammadifar, and Zargaraan (2010) also reported that 1% bassorin dispersion at 25 °C showed a high viscosity gel like structure whereas tragacanthin solution behaved like semi dilute to concentrated solution of entangled, random coil polymers. Therefore, traganthin and bassorin polysaccharides of GT contribute to the swelling power of GT differently. The sugar composition of GT includes mainly galacturonic acid, xylose, fucose, arabinose, galactose, glucose and traces of rhamnose. The presence of these sugars, especially galactose and arabinose residues, contributed to the liquid character of GT (Balaghi, Mohammadifar, Zargaraan, Gavlighi, & Mohammadi, 2011). The low SR of GT, which is very close to C samples, can be attributed to the presence of tragacanthin in the GT samples. The bassorin part of GT provided the gel like characteristics of GT but that was not enough to attain higher SR than C samples.

3.2. Release profiles

Cumulative BC release profiles were determined for both CV and MW hydrogels. Fig. 2 illustrates the CV release profile of hydrogels. According to Fig. 2 all CV heated samples exhibited a similar release profile up to 6 h of the experiment. The distinction in release percentages appeared between the 6 and the 24 h of the experiment. The release percentages of PC, XN and GT samples (37.15%, 32.79% and 29.39%, respectively) were lower than the C samples having 77.81% release at the end of 24 h ($p < 0.05$). Although XN samples had the highest SR, XN hydrogels could also retard the BC release significantly at the end of 24 h, compared to C samples. Generally, hydrogels having high SRs are expected to have high release rates (Oztop & McCarthy, 2011). But, XN hydrogels exerted an opposite behavior. Properties of BC, XN structure and the release medium played a crucial role in the retarded release profile of XN hydrogels. BC having a pH of 3.42 reduced the hydrogel solution pH with respect to hydrogel solutions prepared without BC addition (Table 2). It was hypothesized that, BC entrapment within hydrogels could have provided further crosslinking between the extract and the gel internal structure through electrostatic attractions which should further be confirmed by FTIR experiments. XN and GT hydrogel solutions had the highest pH values compared to other hydrogel solutions whether the solution contained BC or not ($p < 0.05$). The negatively charged branches of XN then believed to interact with the protons coming from the BC led to slow down the release rate. Hydrogen bonding between anthocyanins and the internal gel structure is also important in release since more hydrogen bonding between the encapsulated agent and the polysaccharide gel retards the release rate of the agent (Ferreira, Faria, Grosso, & Mercadante, 2009). The long, branched, complex and strongly negative nature of XN side chains probably increased the hydrogen bonding of BC pigments to the XN gel structure. The slow release of BC from XN hydrogels is also related to the enhanced helical chain entanglement of XN coils which is a common phenomenon for XN molecules (Garcia-Ochoa et al., 2000). The ionic nature of the phosphate buffer medium is another factor contributing to the retarded release rates of XN samples since the salts that are used to prepare buffer solutions tend to strengthen the intermolecular associations between XN molecules (Braga, Azevedo, Marques, Menossi, & Cunha, 2006). As XN hydrogels spend more time in the buffer solution during release experiment, screening of electrostatic repulsion of the trisaccharide side chains occurs and a helical backbone conformation takes place. These phenomena increased the XN gel strength thus decreased the release rate of BC. PC and GT hydrogels also provided a delayed release profile as XN hydrogels did and due to their low SR, their low release rates were expected contrary to XN hydrogels. The formation of junction zones between the WP and the added PC or GT polysaccharide as well as the formation of a three dimensional gel network were clearly

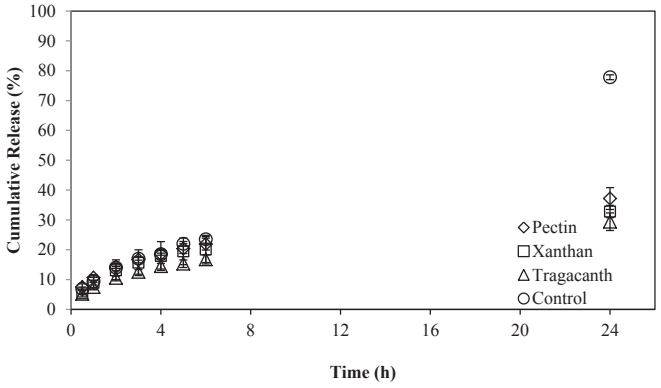

Fig. 2. Release profile of conventionally heated hydrogels (0–24 h).

Table 2
pH values of hydrogel solutions with and without black carrot extract addition. Errors are reported as the standard deviation between replicates. Different small letters mean hydrogel types differed significantly ($p < 0.05$). Different capital letters means addition of black carrot extract reduced the pH of hydrogel solutions significantly ($p < 0.05$).

Hydrogel Solutions	pH with BC	pH without BC
Xanthan	$5.892 \pm 0.039^{a,A}$	$7.046 \pm 0.025^{a,B}$
Tragacanth	$5.820 \pm 0.041^{a,C}$	$7.020 \pm 0.036^{a,D}$
Control	$5.721 \pm 0.038^{b,E}$	$6.946 \pm 0.005^{b,F}$
Pectin	$5.667 \pm 0.021^{b,E}$	$6.828 \pm 0.022^{c,G}$

achieved by these hydrogels. The presence of water soluble part in GT and the high hydrophilicity of GT side residues such as D-xylose, L-fucose and D-galactose increased the interactions between the absorbed water and the GT hydrogel. So, BC molecules were in competition with water molecules to interact with the WPI-GT gel complex. Unlike in XN samples, BC pigments were not particularly preferred over water molecules by GT hydrogel internal structure and this resulted in a similar BC release profile from GT hydrogels to XN hydrogels. A rapid decrease in the viscosity of tragacanthin was reported with the increase in the solution temperature and this also affected the release behavior of GT hydrogels since in CV, hydrogel solutions were heated at 90 °C for 30 min (Mohammadifar, Musavi, Kiumarsi, & Williams, 2006). C samples having the lowest viscosity value showed the fastest release profile suggesting that low viscosity of solutions are associated with the high release rates. The reduced number of junction zones and interactions within the gel matrix in the absence of a polysaccharide also led to a high release rate for C samples. The reasons for release retardation from PC hydrogels are similar to GT case. PC mainly derives its negative charge at pH values higher than its pKa (2.9–3.2) from carboxylate groups like GT which has a pKa value around 3.0 (Nur, Ramchandran, & Vasiljevic, 2016; Ventura & Bianco-Peled, 2015). At pH 7.0, both polysaccharides are strongly negatively charged so that electrostatic and steric repulsions between the side chains played a crucial role in the release of encapsulated compound. Moreover, high hydrophilicity of PC branches contributed to the frequency of water-polysaccharide interactions resulting in diminished BC-polysaccharide interactions. However, this condition was not observed in XN hydrogels. On the contrary, BC molecules sufficiently interacted with XN molecules to slow down the release process despite the high SR which is a driving force for faster release behavior. The difference originates from the more compact and complex conformation of XN molecules (MW of 2000 kDa) than PC (MW of 150 kDa) and GT (MW of 850 kDa) molecules (Mohammadifar et al., 2006; Mohnen, 2008; Zasypkin et al., 1996). Side chain repulsions are also present in XN structure but rigid, close and complex conformation of XN molecules increased interaction sites within the gel network. As a result, XN molecules triggered local aggregate formations in WPI continuous network (Li, Eleya, & Gunasekaran, 2006). This provided a chance for BC molecules to be able to interact with the surrounding polymer network via more hydrogen bonding and electrostatic attractions so, the high SR characteristic of XN hydrogels was overwhelmed by aforementioned conditions and BC release from XN hydrogels was retarded.

Other than the type of the polysaccharide used, variations in the heating rate and mechanism are also important in obtaining hydrogels having different release properties since heating rate and mechanism affect the rheological and polymer interaction properties of hydrogels (Li et al., 2006). For that purpose, the release profiles of MW hydrogels were studied and compared with CV hydrogels. IR assisted MW heating had a distinct effect on release behaviors of hydrogels as shown in Fig. 3. The first two striking

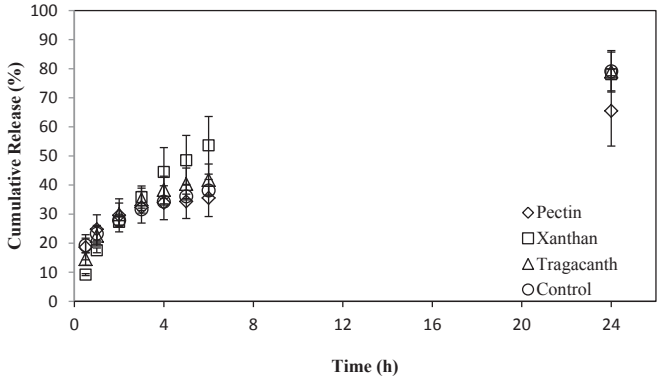

Fig. 3. Release profile of microwave heated hydrogels (0–24 h).

marks in Fig. 3 were the steep increase of the release rates in the early stages of the release experiment and higher final release percents at the end of 24 h with respect to CV samples. The release rates of all hydrogels were similar throughout the experiment and did not show any significant difference in each other ($p > 0.05$). At the end of 24 h, GT, XN, PC and C samples had very close release rates 79.05%, 78.09%, 65.49% and 79.12%, respectively. This result suggests that under MW, release retarding property of polymer added hydrogels was eliminated. Moreover, the distinct release profiles coming from polysaccharide addition was also eliminated. All samples except for PC, started to show increase in the release rate from the 3rd h. After 6 h, each sample, including PC, showed another distinctive increase up to 24 h. In CV, samples showed their first distinctive increase in release rates starting from the 6th h of the experiment. Obviously, MW weakened the gel structures and promoted structural defects within the hydrogels leading to faster release rates. The final release rates of MW samples indicated that all polysaccharide added hydrogels attained higher release rates than their CV counterparts ($p < 0.05$). Although C samples had a higher release rate percent compared to CV the increase was not significant ($p > 0.05$). In addition, from the 2 nd h of the experiment, C samples showed a similar release profile to their CV correspondents. The mechanisms and heating rates of CV and MW are different. MW has a higher heating rate and the heating mechanism depends on electromagnetic field variations causing instantaneous heat generation because of the polarization of the chemical constituents within the material (Liu & Kuo, 2011). On the other hand, CV provides heating by means of thermal conduction with a slower heating rate, thus longer heating times. MW heating provides fast gelling protein solutions close to the isoelectric point of the protein used. The reduction in heating time induces weaker, less homogenous and coagulate-like structures in hydrogels since time to form a three-dimensional gel matrix is decreased (Gustaw & Mleko, 2007). Gustaw and Mleko (2007) reported that at pH 7.0, the difference in microstructures between CV and MW WPI gels were distinct. For instance, MW samples had larger pores than the CV samples. Protein denaturation via protein unfolding or protein subunit dissociation and exposing of hydrophobic parts of the proteins during gelation are common for both types of heating mechanisms. But, CV leads to secondary aggregation after initial protein unfolding. This event contributes to stronger interactions in the gel network and higher gel strength. MW disrupts protein disulfide bonds and gives rise to free sulfhydryl groups quickly. As the MW time elapses these free sulfhydryl groups induce subunit disaggregations leading to a more coagulate-like structure within the gels since MW times are not long enough for crosslinking of these groups. MW also increases the exposure of hydrophobic core residues promoting more protein disaggregation and unfolding. In

contrast to MW, CV does not contribute to the disruption of disulfide bonds but rather enhances the crosslinking of free sulfhydryl groups. Consequently, CV generates WPI hydrogels with strong S–S bonds, enhanced hydrophobic interactions between molecules with a more compact and uniform gel network (Bi et al., 2015). MW release results imply that presence of polysaccharides in WPI hydrogels did not have any effect on release retardation. Their contribution to controlled release completely vanished. The reason for the relatively small difference between CV and MW release rates of C samples compared to other hydrogels originates from the almost complete release of encapsulated compound from the gel matrix at the end of 24 h since hydrogels were stable in that time interval. The removal of remaining small amount of BC was possible after the partial degradation of the hydrogels because remaining BC molecules were strongly bonded to the internal gel structure. Since C hydrogels almost reached the maximum possible release amount even in CV, their release rate enhancement in MW was lower than other hydrogels.

3.3. NMR relaxometry results

NMR relaxometry enables non-destructive analysis of proton relaxation profiles of samples. Analysis of proton relaxation in food systems and hydrogels was utilized to obtain information about the internal structure of the samples (Oztop et al., 2014). T_2 constant which is also represented as spin-spin relaxation time, is a useful parameter to interpret the water-polymer and polymer-polymer interactions in a gel system. The presence of water in such samples gives rise to T_2 since liquid materials has higher T_2 than solid materials. The reason is that in liquids, protons are located further apart compared to protons of solid materials having a closely packed conformation. So, protons in solid substances dephase faster than liquid protons, after the 90° radio frequency pulse is turned off, giving lower T_2 values (Hashemi, Bradley, & Lisanti, 2010).

Hydrogel T_2's was measured before the solvent immersion of the gels and through the one day solvent uptake experiment. Initially, before solvent uptake, XN hydrogels had the lowest T_2 (50.61 ms) of all the hydrogels (Fig. 4). Beginning from the 2 nd h of the swelling experiment, all CV samples showed similar T_2 values throughout the experiment. Therefore, 24 h T_2 profiles of each sample were investigated, separately. XN hydrogels presented a significant T_2 increase between the 6th and the 24th h of the experiment ($p < 0.05$). This increase in T_2 is in consistence with the high SR of XN at the end of 24 h. The main factors contributing to the increase in T_2 of XN samples are amount of water present in XN gels and the water-gel network interactions in XN hydrogels. XN samples absorbed larger amount of solvent than C samples, and this led to larger T_2. The increase in the amount of water thus hydrogen molecules results in larger T_2 values (Oztop, Rosenberg, Rosenberg, McCarthy, & McCarthy, 2010). Another reason is the abundance of BC-polymer interactions in XN hydrogels. BC molecules interacted with the XN gel matrix more than with other hydrogel matrices as previously mentioned. This event reduced the water-polymer interactions in the XN gel matrix. A considerable amount of absorbed water then remained in free state leading large T_2 values. C samples indicated a significant increase in T_2 starting from 2 h but this tendency did not continue. Moreover, at 24 h, T_2 of C samples experienced a fall making the final T_2 analogous to initial T_2 of the C hydrogels. Although C samples noticeably swelled during the 24 h experiment, their high BC release rate affected the solvent-polymer interactions in the gels. Removal of excess amount of BC from C gel matrix through the end of the experiment provoked more water-polymer interactions within the hydrogel. The interaction sites of the C gel network were more available for water molecules after the release of BC. PC and GT hydrogels also exhibited a considerable SR ($p < 0.05$) but they did not show an important T_2 increase at any time of the solvent uptake. Normally, a major increase in SR should provide also a major increase in T_2 values since the higher amount of solvent present in the hydrogels increases T_2 values. In the case of PC and GT hydrogels, absorbed water interacted with the surrounding environment in much more abundance with respect to water-polymer interactions in other hydrogels. The highly hydrophilic nature of side chains of both polysaccharides was discussed in the release section. Despite the amount of solvent increased in these hydrogels, water-polymer interactions predominated and hold T_2 stable over the swelling period.

IR assisted MW had a crucial impact on the T_2 profiles of the hydrogels (Fig. 5). T_2 values of PC and GT hydrogels started to show an increase from the 2 nd h of the experiment whose T_2 profiles were stable throughout the experiment in CV. XN hydrogels which had also a stable T_2 profile until the end of 6 h in CV samples, experienced an increase in T_2 beginning from 4 h. C hydrogels exerted similar T_2 profile to their CV T_2 analogues but their MW samples showed decrease in T_2 at the 4 h of the experiment. The same tendency was observed at the 24 h in CV. Although T_2 values of MW and CV samples were similar to each other for each time interval except for the beginning of the experiment, the distinct changes in the T_2 profiles of MW hydrogels explain that the water-polymer interactions and the behaviors of solvent within hydrogels were clearly altered by MW. Since an increasing tendency of T_2 times were observed in all samples, it is claimed that MW hydrogels had weaker gel structures during water uptake allowing water molecules to present in free state diffusing in and out through the

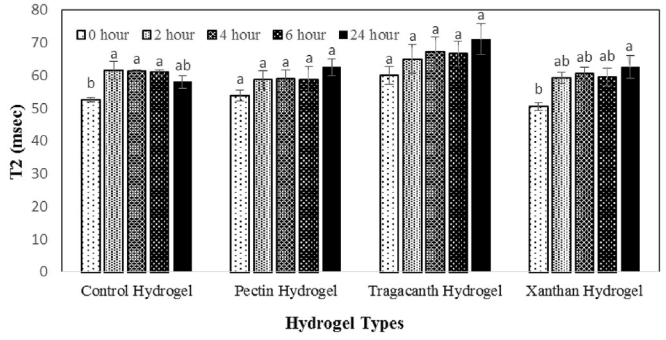

Fig. 4. T_2 results of conventionally heated hydrogels. Errors are reported as the standard error between replicates. Different letters mean T_2 of hydrogel samples differed significantly ($p < 0.05$). (ANOVA results represent T_2 changes for 24 h experiment. Letterings were conducted for each hydrogel group separately).

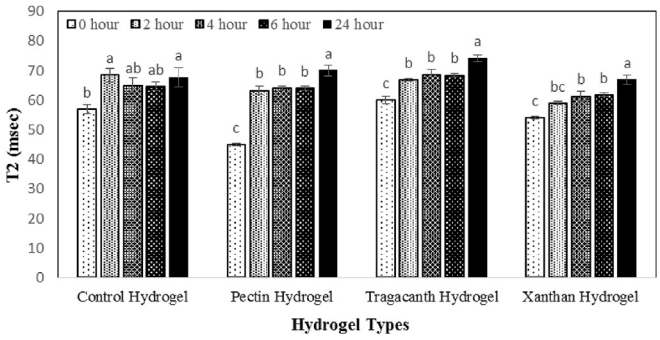

Fig. 5. T_2 results of infrared assisted microwave heated hydrogels. Errors are reported as the standard error between replicates. Different letters mean T_2 of hydrogel samples differed significantly ($p < 0.05$). (ANOVA results represent T2 changes for 24 h experiment. Letterings were done for each hydrogel group separately).

hydrogels.

SDC of water in hydrogels were determined to further investigate the gel properties of CV and MW samples. SDC of water molecules (m^2/s) in the hydrogels were determined by NMR and the obtained SDC values represented the average values of the SDC of water molecules coming from different compartments within the hydrogels as shown in Tables 3 and 4. Additionally, in order to see the change in SDC values for different heating types, results were displayed in Figs. 6–7. Proton relaxation times provide information about the water content of hydrogels but since there are many protons coming from different materials within the hydrogels such as the macromolecular surroundings, the direct SDC measurement of water can be introduced for more specific findings. The mobility of water protons and their self-diffusion throughout the matrix can be detected by SDC measurements. The SDC of water is influenced by the presence of polymers. The SDC of water is reduced by the increase in the water-polymer interactions (Manetti, Casciani, & Pescosolido, 2004). CV hydrogels revealed close SDC results before water uptake. After 6 h of solvent immersion, all CV hydrogels except for C experienced an increase in their SDCs (Fig. 6). This increase in SDC was directly related to the water uptake of these hydrogels. As the amount of water absorbed increased, SDC of that hydrogel increased as well. Solvent uptake did not alter the SDC of C samples which was consistent with the lowest SR of CV C samples. The increased polymer-water interaction hypothesis for CV C samples were supported by the low and stable SDC values of these samples. In addition, the SDC value of CV XN hydrogel (1.67 m^2/s) was significantly higher than C hydrogels (1.45 m^2/s) at 6 h ($p < 0.05$). The PC and GT SDC values attained intermediate values 1.57 and 1.51 m^2/s, respectively. These SDC results were identical to SR results, in terms of statistical analysis, claiming that SR plays a crucial role on the SDC values. MW hydrogels, contrary to CV hydrogels, did not show such an increase in their SDC values at the end of 6 h of solvent uptake process (Fig. 7). Moreover, there were no difference in SDCs of different MW hydrogels for both the beginning and the 6 h of the measurements. The stability in the MW hydrogel SDC values implies that unlike CV hydrogels, MW hydrogels were not capable of retaining sufficient amount of water in their gel structures to form a proper gel matrix. In addition to the SDC analysis for each heating type, the comparison of CV and MW hydrogel SDC values was also performed. After 6 h of solvent uptake, only the SDC of CV XN hydrogels was higher than their MW counterparts ($p < 0.05$) (Table 4). This result points out the fact that CV XN hydrogels, having high SR and low release rate, were the most severely affected hydrogels by the IR assisted MW.

3.4. Dielectric properties

Dielectric constant (ε') and dielectric loss factor (ε'') of a food determine the MW characteristics of these products. ε' describes the ability of a material to store microwave energy. ε'' is the ability of a material to dissipate this microwave energy into heat (Sakiyan, Sumnu, Sahin, & Meda, 2007). Dielectric properties of hydrogel solutions showed variations as shown in Table 5. GT solutions had lower dielectric properties with respect to other polysaccharide solutions which contributed to the more homogenous MW heating due to the increased penetration depth (Calay, Newborough, Probert, & Calay, 1995). The reason could be the water soluble (tragacanthin) part of the GT. The close ε'' of GT solutions to distilled water implies that the MW properties of GT solutions are closer to distilled water than that of others. The lowest ε' of GT solution also suggests that GT binds water efficiently leaving less free water to increase the ε' of the solution. Therefore, the more stable T_2 profile of GT hydrogels compared to other hydrogels can also be associated with its dielectric properties. When the ε'' of XN, C and PC solutions were examined, it is clear that these polysaccharides induced faster heating rates in MW than GT solutions. One of the most radical increases in release rates were observed for MW XN hydrogels as previously mentioned. The high ε'' of XN probably contributed to the high release in MW XN hydrogels since even a small increase in the heating rate can cause abrupt changes such as increased pore size in the gel network (Li et al., 2006).

Table 3
SDC values of CV and MW hydrogels for 0 h. Errors are reported as the standard deviation between replicates. Different small letters mean hydrogel types differed significantly in each column ($p < 0.05$). Different capital letters mean heating type affected the SDC values significantly ($p < 0.05$).

Hydrogel Type	CV SDC 0 h (m^2/s)	MW SDC 0 h (m^2/s)
Xanthan	$1.349\pm 0.044^{a,A}$	$1.250\pm 0.013^{a,A}$
Tragacanth	$1.391\pm 0.031^{a,A}$	$1.226\pm 0.042^{a,B}$
Control	$1.329\pm 0.020^{a,A}$	$1.259\pm 0.040^{a,A}$
Pectin	$1.389\pm 0.002^{a,A}$	$1.278\pm 0.073^{a,A}$

Table 4
SDC values of CV and MW hydrogels. Errors are reported as the standard deviation between replicates. Different small letters mean hydrogel types differed significantly in each column ($p < 0.05$). Different capital letters mean heating type affected the SDC values significantly ($p < 0.05$).

Hydrogel Type	CV SDC 6 h (m^2/s)	MW SDC 6 h (m^2/s)
Xanthan	$1.676\pm 0.044^{a,A}$	$1.348\pm 0.032^{a,B}$
Tragacanth	$1.516\pm 0.023^{ab,A}$	$1.390\pm 0.052^{a,A}$
Control	$1.452\pm 0.078^{b,A}$	$1.389\pm 0.056^{a,A}$
Pectin	$1.574\pm 0.046^{ab,A}$	$1.380\pm 0.126^{a,A}$

3.5. Release modelling of hydrogels

Mathematical modelling of release of BC from gels was performed using Fick's second law. Release data were fitted to analytical solution given in Eq. (2) to obtain best estimated value for diffusivity, D, using MATLAB nonlinear curve fitting subroutine.Several factors such as composition of hydrogel (polymer type, etc.), preparation technique, geometry of gel (shape and size), environmental conditions during release influence release behavior (Zarzycki, Modrzejewska, & Nawrotek, 2010). Exterior diffusion, interior diffusion, desorption and chemical reactions are among the release mechanisms. In this study, swelling ratio has risen up to maximum 17.85% and diffusion controlled mechanism has been considered. Thus, interior diffusion throughout polymeric matrix has been explained by Fick's second law of diffusion. All fitted values of diffusion coefficients for all formulations were given in Table 6. A representative plot of both experimental and model data was displayed on Fig. 8. D values for BC release from gel samples were found in the order of 10^{-10} m^2/s. The results varied between 0.59×10^{-10} and 1.78×10^{-10} m^2/s. No significant difference was obtained between samples ($p > 0.05$).

3.6. Microstructures of hydrogels

SEM images of hydrogel samples revealed that the addition and the type of polysaccharide used affected the gel microstructures. In addition to polysaccharide addition, CV and MW brought striking characteristic microstructural differences in gel matrices (Fig. 9). Firstly, all MW images showed a smoother and a more coagulate like structures with respect to their CV correspondents. CV C hydrogels had a homogenous honeycomb like gel structure whereas CV PC and XN hydrogels possessed more clumpy and

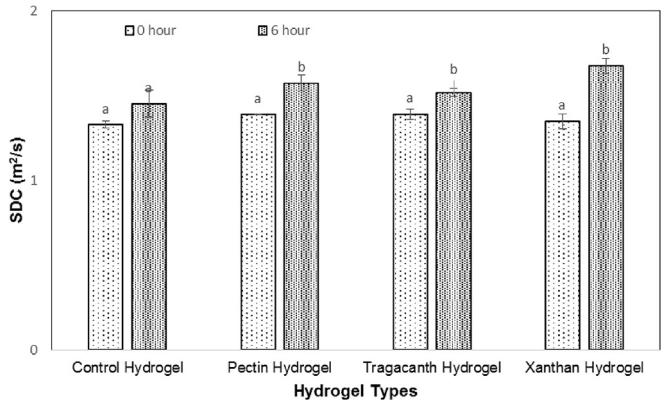

Fig. 6. SDC results of conventionally heated hydrogels. Errors are reported as the standard error between replicates. Different letters mean SDC of hydrogel samples differed significantly ($p < 0.05$). (ANOVA results represent SDC changes for 0 h and 6 h experiment. Letterings were done for each hydrogel group separately).

dense structures. Local aggregates could also be observed in CV PC and CV XN hydrogels indicating high cross-link density in these samples. CV GT hydrogels, in contrast to other CV samples, exhibited a smooth, sheet like gel network which was close to MW images. The gel network properties of CV GT justified the stable T2 profile of GT hydrogels. CV XN hydrogels had a homogenous distribution of local aggregates. These closely packed and clumpy structure of CV XN hydrogels provided these hydrogels a high water holding capacity. The microstructure of CV XN samples validated the high SR in swelling experiments. PC samples were similar to XN samples but the distribution of aggregates were more heterogeneous and the size of the aggregates were bigger than the ones in XN hydrogels. This also caused a more porous structure for CV PC hydrogels. When MW image of C samples were examined it was observed that MW increased the pore size of the gel and the particulates within the gel network became milder. The effect of MW was more severe on the PC and XN hydrogels. The clumpy and dense structures of these gels were lost after MW. The dramatic increase in the release rates of MW XN and PC hydrogels was justified by the dramatic change of the microstructures of their images by the heating type. XN hydrogels were clearly subjected to most severe alterations in the gel structure after MW. The slight differences between the CV GT and MW GT hydrogel images are attributed to the water interaction properties of GT polymer. GT has

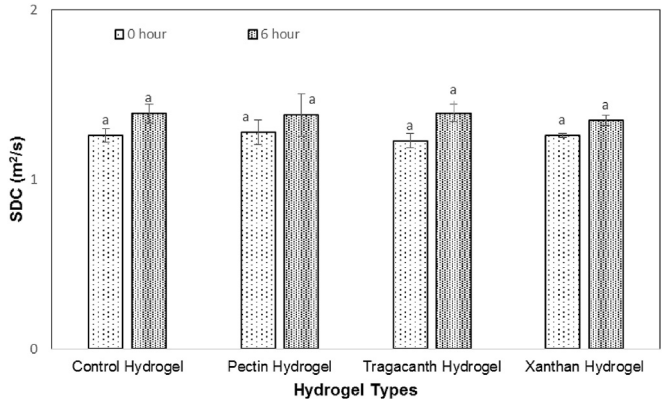

Fig. 7. SDC results of infrared assisted microwave heated hydrogels. Errors are reported as the standard error between replicates. Different letters mean SDC of hydrogel samples differed significantly ($p < 0.05$). (ANOVA results represent SDC changes for 0 h and 6 h experiment. Letterings were done for each hydrogel group separately).

Table 5
Dielectric properties of hydrogel solutions. Errors are reported as the standard deviation between replicates. Lettering was done for each column and different letters mean significant difference between hydrogel solutions ($p < 0.05$).

Hydrogel Solutions	Dielectric Constant (ε')	Dielectric Loss Factor (ε'')
Distilled Water	77.868± 0.8280[a]	9.5906± 0.2157[c]
Xanthan	60.537± 1.6052[b]	13.8288± 0.3042[a]
Control	60.122± 0.8735[b]	13.5953± 0.2248[a]
Pectin	59.739± 1.2937[bc]	13.5463± 0.3428[a]
Tragacanth	55.664± 0.6519[c]	12.4176± 0.1349[b]

Table 6
Diffusion coefficients of gel samples. Results are mean values and errors are represented as standard deviation for at least two replicates in each gel sample.

	D (m^2/s)	R^2
CV Hydrogels		
Pectin	$(1.39 \pm 0.35) \times 10^{-10}$ [a]	≥0.96
Xanthan	$(2.29 \pm 1.52) \times 10^{-10}$ [a]	≥0.95
Tragacanth	$(1.13 \pm 0.03) \times 10^{-10}$ [a]	≥0.96
Control	$(0.59 \pm 0.18) \times 10^{-10}$ [a]	≥0.96
IR-MW Hydrogels		
Pectin	$(1.53 \pm 0.08) \times 10^{-10}$ [a]	≥0.96
Xanthan	$(1.17 \pm 0.33) \times 10^{-10}$ [a]	≥0.93
Tragacanth	$(1.53 \pm 1.37) \times 10^{-10}$ [a]	≥0.87
Control	$(1.18 \pm 0.49) \times 10^{-10}$ [a]	≥0.86

a high affinity for water and water soluble part of the GT molecular structure contributes to coagulate like structure of the respective hydrogels. MW also induced even a more coagulate like structure of GT and this is in accordance with the low dielectric properties of GT hydrogels.

4. Conclusions

Polymer addition to BC containing composite WPI hydrogels and heating type for gelation revealed distinct SR, release profiles and gel microstructure properties. CV XN hydrogels were the only samples having higher SR than CV C hydrogels. CV PC, XN and GT hydrogels showed a retarded release profile compared to C hydrogels in pH 7.0 phosphate buffer solution at the end of 24 h. IR assisted MW was introduced in this study as a new approach for obtaining composite WPI hydrogels. MW induced microstructural changes in the gel networks thus, higher release rates for all hydrogels except for C. Investigation of release profiles of WPI-GT hydrogels is believed to be crucial due to rare information on the subject in literature. This study also presented the MW release behavior of WPI-GT composite hydrogels for the first time. GT

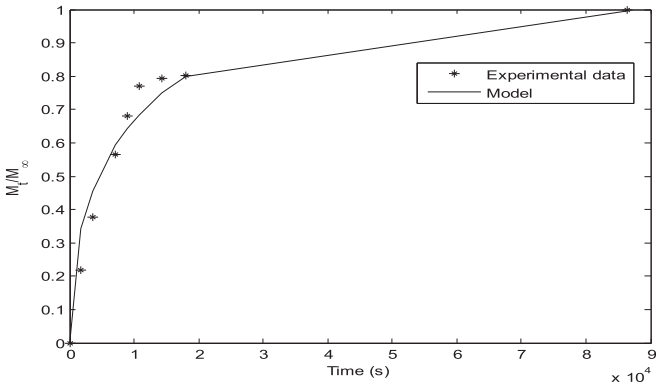

Fig. 8. Representative fitting model of conventional XN gel for both experimental and model data ($R^2 \geq 0.95$).

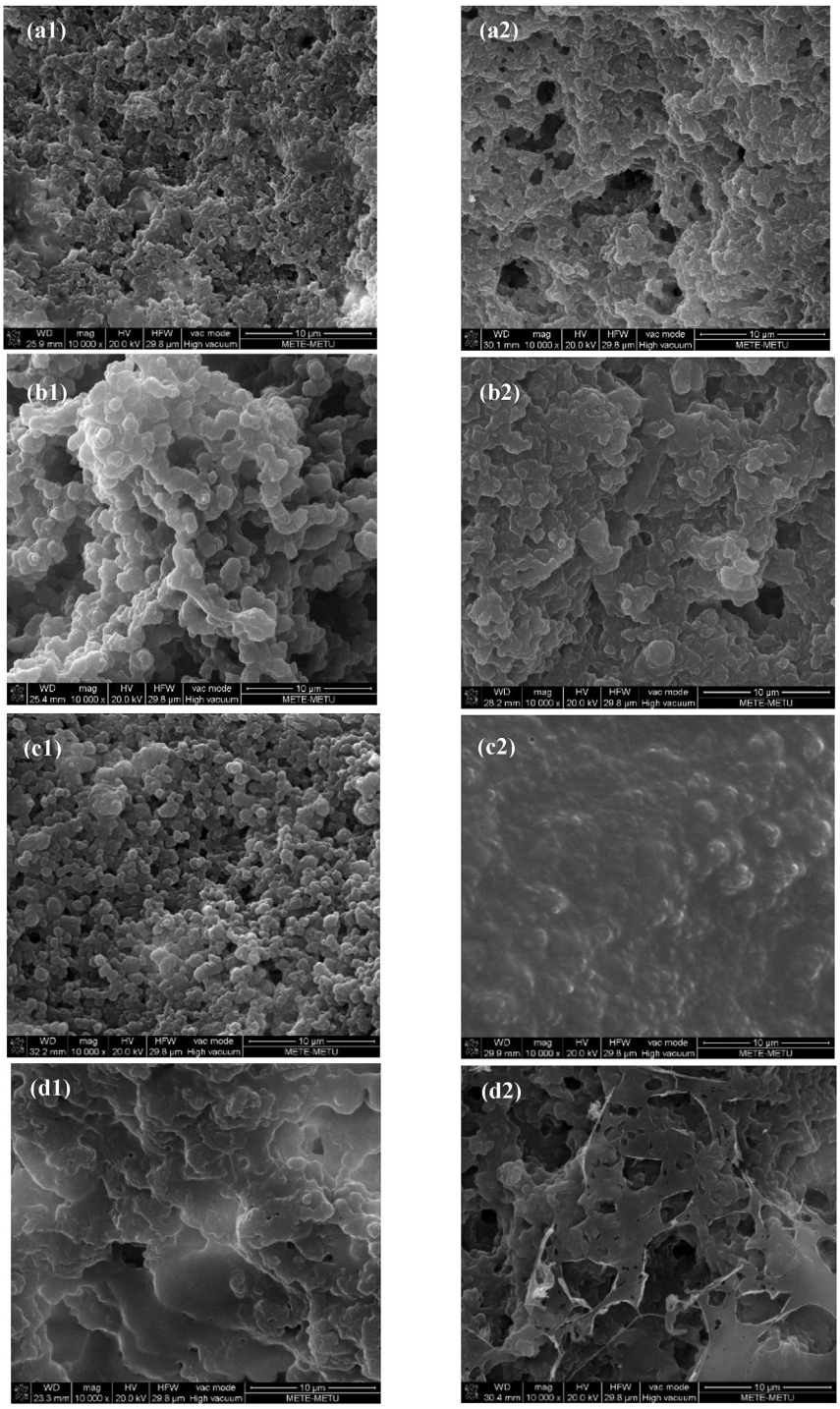

Fig. 9. SEM images of hydrogels. (a1) CV C; (a2) MW C; (b1) CV PC; (b2) MW PC; (c1) CV XN; (c2) MW XN; (d1) CV GT; (d2) MW GT.

hydrogels showed coagulated structure rather than a highly cross-linked gel network for both CV and MW samples. T_2 and SDC of each hydrogel were evaluated. T_2 provided further information about the water-polymer interactions and better gelling properties are associated with the increase in T_2. SDC values were found to be increased by the increase in SR so the increase in the CV XN hydrogel SR was detected by SDC measurements. This study demonstrated that for the desired fast release conditions from hydrogels, MW can be employed for gelation process. The utility of NMR data also indicated that NMR relaxometry can be used to analyze gel swelling and release characteristics. Further studies should focus on MW gelling and various polymer blending to WPI hydrogels in order to achieve better understanding of the release profiles of such hydrogels.

Acknowledgements

The authors would like to thank Prof. Dr. Gulum Sumnu and M. Sc student Mete Kilercioglu from Middle East Technical University Food Engineering Department and Dr. Ozge Sakiyan Demirkol from

Ankara University Food Engineering Department for their valuable contributions to the study.

References

Argin, S., Kofinas, P., & Lo, Y. M. (2014). The cell release kinetics and the swelling behavior of physically crosslinked xanthan-chitosan hydrogels in simulated gastrointestinal conditions. *Food Hydrocolloids, 40*, 138–144.

Aydogdu, A., Sumnu, G., & Sahin, S. (2015). Effects of microwave-infrared combination drying on quality of eggplants. *Food and Bioprocess Technology, 8*, 1198–1210.

Balaghi, S., Mohammadifar, M. A., & Zargaraan, A. (2010). Physicochemical and rheological characterization of gum tragacanth exudates from six species of Iranian Astragalus. *Food Biophysics, 5*, 59–71.

Balaghi, S., Mohammadifar, M. A., Zargaraan, A., Gavlighi, H. A., & Mohammadi, M. (2011). Compositional analysis and rheological characterization of gum tragacanth exudates from six species of Iranian Astragalus. *Food Hydrocolloids, 25*(7), 1775–1784.

Belscak-Cvitanovic, A., Dordevic, V., Karlovic, S., Pavlovic, V., Komes, D., Jezek, D., et al. (2015). Protein-reinforced and chitosan-pectin coated alginate microparticles for delivery of flavan-3-ol antioxidants and caffeine from green tea extract. *Food Hydrocolloids, 51*, 361–374.

Betz, M., & Kulozik, U. (2011a). Microencapsulation of bioactive bilberry anthocyanins by means of whey protein gels. *Procedia Food Science, 1*, 2046–2056.

Betz, M., & Kulozik, U. (2011b). Whey protein gels for the entrapment of bioactive anthocyanins from bilberry extract. *International Dairy Journal, 21*(9), 703–710.

Betz, M., Steiner, B., Schantz, M., Oidtmann, J., Mader, K., Richling, E., et al. (2012). Antioxidant capacity of bilberry extract microencapsulated in whey protein hydrogels. *Food Research International, 47*(1), 51–57.

Bi, W., Zhao, W., Li, X., Ge, W., Muhammad, Z., Wang, H., et al. (2015). Study on microwave-accelerated casein protein grafted with glucose and β-cyclodextrin to improve the gel properties. *International Journal of Food Science & Technology, 50*(6), 1429–1435.

Braga, A. L. M., Azevedo, A., Marques, M. J., Menossi, M., & Cunha, R. L. (2006). Interactions between soy protein isolate and xanthan in heat-induced gels: The effect of salt addition. *Food Hydrocolloids, 20*, 1178–1189.

Buffler, C. (1993). *Microwave cooking and processing: Engineering fundamentals for the food scientist*. New York: Avi Book.

Calay, R. K., Newborough, M., Probert, D., & Calay, P. S. (1995). Predictive equations for the dielectric properties of foods. *International Journal of Food Science and Technology, 29*, 699–713.

Crank, J. (1975). *The mathematics of diffusion* (2nd ed.). London: Oxford University Press.

Cussler, E. L. (2009). *Diffusion: Mass transfer in fluid systems. Engineering* (3rd ed.). Cambridge University Express (Chapter 5).

Déat-lainé, E., Hoffart, V., Garrait, G., Jarrige, J., Cardot, J., Subirade, M., et al. (2013). Efficacy of mucoadhesive hydrogel microparticles of whey protein and alginate for oral insulin delivery. *Pharm. Res., 30*, 721–734.

Ferreira, D. S., Faria, A. F., Grosso, C. R. F., & Mercadante, A. Z. (2009). Encapsulation of blackberry anthocyanins by thermal gelation of curdlan. *Journal of the Brazilian Chemical Society, 20*(10), 1908–1915.

Garcia-Ochoa, F., Santos, V. E., Casas, J. A., & Gomez, E. (2000). Xanthan gum: Production, recovery, and properties. *Biotechnology Advances, 18*, 549–579.

Gunasekaran, S., Ko, S., & Xiao, L. (2007). Use of whey proteins for encapsulation and controlled delivery applications. *Journal of Food Engineering, 83*(1), 31–40.

Guo, J., & Kaletunc, G. (2016). Dissolution kinetics of pH responsive alginate-pectin hydrogel particles. *Food Research International* (this volume).

Gustaw, W., & Mleko, S. (2007). Gelation of whey proteins by microwave heating. *Milchwissenschaft-Milk Science International, 62*, 439–442.

Hashemi, R. H., Bradley, W. G., & Lisanti, C. J. (2010). *MRI: The Basics* (3rd ed.). Philadelphia: Lippicott Williams & Wilkins (Chapter 4).

Hatami, M., Nejatian, M., Mohammadifar, M. A., & Pourmand, H. (2014). Milk protein – gum tragacanth mixed gels: Effect of heat-treatment sequence. *Carbohydrate Polymers, 101*, 1068–1073.

Khandare, V., Walia, S., Singh, M., & Kaur, C. (2011). Black carrot (Daucus carota ssp. sativus) juice: Processing effects on antioxidant composition and color. *Food and Bioproducts Processing, 89*(4), 482–486.

Kim, B., Flamme, K. La, & Peppas, N. A. (2002). Dynamic swelling behavior of pH-sensitive anionic hydrogels used for protein delivery. *Journal of Applied Polymer Science, 89*, 1606–1613.

Kirca, A., Ozkan, M., & Cemeroglu, B. (2006). Stability of black carrot anthocyanins in various fruit juices and nectars. *Food Chemistry, 97*, 598–605.

Lee, S. J., & Rosenberg, M. (2000). Whey protein-based microcapsules prepared by double emulsification and heat gelation. *LWT - Food Science and Technology, 33*(2), 80–88.

Leon, A. M., Medina, W. T., Park, D. J., & Aguilera, J. M. (2016). Mechanical properties of whey protein/Na alginate gel microparticles. *Journal of Food Engineering, 188*, 1–7.

Le, X. T., Rioux, L., & Turgeon, S. L. (2016,). Formation and functional properties of protein – polysaccharide electrostatic hydrogels in comparison to protein or polysaccharide hydrogels. *Advances in Colloid and Interface Science, 239*, 127–135.

Li, J., Eleya, M. M. O., & Gunasekaran, S. (2006). Gelation of whey protein and xanthan mixture: Effect of heating rate on rheological properties. *Food Hydrocolloids, 20*, 678–686.

Lin, C. C., & Metters, A. T. (2006). Hydrogels in controlled release formulations: Network design and mathematical modeling. *Advanced Drug Delivery Reviews, 58*(12–13), 1379–1408.

Liu, H. H., & Kuo, M. I. (2011). Effect of microwave heating on the viscoelastic property and microstructure of soy protein isolate gel. *Journal of Texture Studies, 42*(1), 1–9.

Lu, M., Li, Z., Liang, H., Shi, M., Zhao, L., Li, W., et al. (2015). Controlled release of anthocyanins from oxidized konjac glucomannan microspheres stabilized by chitosan oligosaccharides. *Food Hydrocolloids, 51*, 476–485.

Luqin, S., Zhao, Y., Huang, J., Sha, L., Zhai, X., & Gao, L. (2009). Calcium pectinate gel bead intended for oral protein delivery: Preparation improvement and formulation development. *Chemical & Pharmaceutical Bulletin, 57*, 663–667.

Manetti, C., Casciani, L., & Pescosolido, N. (2004). LF-NMR water self-diffusion and relaxation time measurements of hydrogel contact lenses interacting with artificial tears. *Journal of Biomaterial Science, 15*(3), 331–342.

McClements, D. J. (2017). Recent progress in hydrogel delivery systems for improving nutraceutical bioavailability. *Food Hydrocolloids, 68*, 238–245.

Mikac, U., Sepe, A., Kristl, J., & Baumgartner, S. (2010). A new approach combining different MRI methods to provide detailed view on swelling dynamics of xanthan tablets influencing drug release at different pH and ionic strength. *Journal of Controlled Release, 145*, 247–256.

Mohammadifar, M. A., Musavi, S. M., Kiumarsi, A., & Williams, P. A. (2006). Solution properties of targacanthin (water-soluble part of gum tragacanth exudate from Astragalus gossypinus). *Biological Macromolecules, 38*, 31–39.

Mohnen, D. (2008). Pectin structure and biosynthesis. *Current Opinion in Plant Biology, 11*(3), 266–277.

Mostafavi, F. S., Kadkhodaee, R., Emadzadeh, B., & Koocheki, A. (2016). Preparation and characterization of tragacanth – locust bean gum edible blend films. *Carbohydrate Polymers, 139*, 20–27.

Munialo, C. D., Linden, van der E., Ako, K., Nieuwland, M., As, H. V., & Jongh, H. H. J. (2016). The effect of polysaccharides on the ability of whey protein gels to either store or dissipate energy upon mechanical deformation. *Food Hydrocolloids, 52*, 707–720.

Mun, S., Kim, Y. R., & McClements, D. J. (2015). Control of β-carotene bioaccessibility using starch-based filled hydrogels. *Food Chemistry, 173*, 454–461.

Nur, M., Ramchandran, L., & Vasiljevic, T. (2016). Tragacanth as an oral peptide and protein delivery carrier: Characterization and mucoadhesion. *Carbohydrate Polymers, 143*, 223–230.

Ozel, B., Uguz, S. S., Kilercioglu, M., Grunin, L., & Oztop, M. H. (July 2016). Effect of different polysaccharides on swelling of composite whey protein hydrogels: A low field (LF) NMR relaxometry study. *Journal of Food Process Engineering*, 1–9.

Oztop, M. H., & McCarthy, K. L. (2011). Mathematical modeling of swelling in high moisture whey protein gels. *Journal of Food Engineering, 106*(1), 53–59.

Oztop, M. H., McCarthy, K. L., McCarthy, M. J., & Rosenberg, M. (2012). Uptake of divalent ions (Mn +2 and Ca +2) by heat-set whey protein gels. *Journal of Food Science, 77*(2), 68–73.

Oztop, M. H., McCarthy, K. L., McCarthy, M. J., & Rosenberg, M. (2014). Monitoring the effects of divalent ions (Mn+2 and Ca+2) in heat-set whey protein gels. *LWT - Food Science and Technology, 56*(1), 93–100.

Oztop, M. H., Rosenberg, M., Rosenberg, Y., McCarthy, K. L., & McCarthy, M. J. (2010). Magnetic resonance imaging (MRI) and relaxation spectrum analysis as methods to investigate swelling in whey protein gels. *Journal of Food Science, 75*(8), 508–515.

Petzold, G., Gianelli, M. P., Bugueño, G., Celan, R., Pavez, C., & Orellana, P. (2014). Encapsulation of liquid smoke flavoring in ca-alginate and ca-alginate-chitosan beads. *Journal of Food Science and Technology, 51*(1), 183–190.

Sakiyan, O., Sumnu, G., Sahin, S., & Meda, V. (2007). Investigation of dielectric properties of different cake formulations during microwave and infrared – microwave combination baking. *Food Engineering and Physical Properties, 72*(4), 205–213.

Shiroodi, S. G., Mohammadifar, M. A., Gorji, E. G., Ezzatpanah, H., & Zohouri, N. (2012). Influence of gum tragacanth on the physicochemical and rheological properties of kashk. *Journal of Dairy Research, 79*, 93–101.

Shiroodi, S. G., Rasco, B. A., & Lo, Y. M. (2015). Influence of xanthan-curdlan hydrogel complex on freeze-thaw stability and rheological properties of whey protein isolate gel over multiple freeze-thaw cycle. *Journal of Food Science, 80*(7), 1498–1505.

Siepmann, J., & Peppas, N. A. (2001). Modeling of drug release from delivery systems based on hydroxypropyl methylcellulose (HPMC). *Advanced Drug Delivery Reviews, 48*(2–3), 139–157.

Sun, J., Chen, M., Wang, H., Jiang, B., Mattea, C., Stapf, S., et al. (2016). PFG-NMR measurement of self-diffusion coefficients of long-chain a -olefins and their mixtures in semi-crystalline polyethylene. *Journal of Applied Polymer Science, 44143*, 2–9.

Tsai, R., Chen, P., Kuo, T., Lin, C., Wang, D., Hsien, T., et al. (2014). Chitosan/pectin/gum Arabic polyelectrolyte complex: Process-dependent appearance, microstructure analysis and its application. *Carbohydrate Polymers, 101*, 752–759.

Turabi, E., Sumnu, G., & Sahin, S. (2010). Quantitative analysis of macro and microstructure of gluten-free rice cakes containing different types of gums baked in different ovens. *Food Hydrocolloids, 24*(8), 755–762.

Ventura, I., & Bianco-Peled, H. (2015). Small-angle X-ray scattering study on pectin-chitosan mixed solutions and thermoreversible gels. *Carbohydrate Polymers, 123*, 122–129.

Wichchukit, S., Oztop, M. H., McCarthy, M. J., & McCarthy, K. L. (2013). Whey protein/alginate beads as carriers of a bioactive component. *Food Hydrocolloids, 33*(1), 66–73.

Williams, P. D., Oztop, M. H., McCarthy, M. J., McCarthy, K. L., & Lo, Y. M. (2011). Characterization of water distribution in xanthan-curdlan hydrogel complex using magnetic resonance imaging, nuclear magnetic resonance relaxometry, rheology, and scanning electron microscopy. *Journal of Food Science, 76*(6), 472–478.

Yang, N., Luan, J., Ashton, J., Gorczyca, E., & Kasapis, S. (2014). Effect of calcium chloride on the structure and in vitro hydrolysis of heat induced whey protein and wheat starch composite gels. *Food Hydrocolloids, 42*, 260–268.

Zand-Rajabi, H., & Madadlou, A. (2016). Caffeine-loaded whey protein hydrogels reinforced with gellan and enriched with calcium chloride. *International Dairy Journal, 56*, 38–44.

Zarzycki, R., Modrzejewska, Z., Nawrotek, K., & Hydrozeli, U. (2010). Drug release from hydrogel matrices. *Ecological Chemistry and Engineering S, 17*(2), 117–136.

Zasypkin, D. V., Dumay, E., & Cheftel, J. C. (1996). Pressure- and heat-induced gelation of mixed β-lactoglobulin/xanthan solutions. *Food Hydrocolloids, 10*(2), 203–211.

Zhang, Z., Decker, E. A., & McClements, D. J. (2014). Encapsulation, protection, and release of polyunsaturated lipids using biopolymer-based hydrogel particles. *Food Research International, 64*, 520–526.